CDF/PHYS/ELECTROWEAK/CDFR/9723
Draft 1.0
April 10, 2010

Measurement of the WZ Diboson Production Cross Section using 5.3 fb^{-1}

Doug Benjamin, Mark Kruse

Duke University

Eric James, Sergo Jindariani, Britney Rutherford

Fermilab

Roman Lysak

IEP SAS, Slovakia

Dean Andrew Hidas

Rutgers University

Aidan Robson, Rick St. Denis, Peter Bussey

University of Glasgow

Matthew Herndon, Jason Nett[1], Jennifer Pursley

University of Wisconsin, Madison

Maria d'Errico, Simone Pagan Griso, Donatella Lucchesi

INFN and University of Padova

Abstract

[1]Contact: Jason Nett jnett@wisc.edu

WZ production is a crucial background to the $H \to WW$ trilepton search. The WZ cross section is measured using the same lepton and event selection as the $H \to WW$ search. A NeuroBayes neural net is used to distinguish WZ signal from backgrounds in the final selection region. The WZ cross section is then extracted using a maximum likelihood method which best fits the neural net score signal and background shapes to the data. This analysis uses up to 5.3 fb^{-1} of CDF Run II data. The measured WZ cross section is $3.63^{+0.89}_{-0.73}$ pb^{-1}, consistent with the 3.46 ± 0.21 pb^{-1} predicted by theory. This is a significant improvement over the previously published result of $5.0^{+1.8}_{-1.6}$ pb^{-1}

Contents

1 Introduction

In this note, we present a measurement of the $WZ \to l\nu, ll$ production cross section using approximately 5.3 fb^{-1} of integrated luminosity. This measurement is an offshoot of the Standard Model $VH \to VWW^* \to$ trilepton $+\not\!\!E_T$ search described in CDF Note 10020 [2], using the same framework. The WZ cross section measurement was first tested using 1.1 fb^{-1} and presented in CDF Note 8659 [5], then later updated–though not published– to 1.9fb^{-1}[8].

For the WZ cross section measurement, we use only events with

- three leptons (e or μ)
- any number of jets
- $\not\!\!E_T > 25.0$GeV
- Z-boson selection (see section 2.3).

In 5.3 fb^{-1} of data, we find 48 events, $\sim$ 36 of which are expected to be WZ events with the rest coming from Standard Model backgrounds. To measure the WZ cross section, we train a NeuroBayes neural network to separate the signal from background. We then form and fit a likelihood ratio for the normalization of WZ events using background templates derived primarily from Monte Carlo samples.

This analysis note proceeds as follows:

1. Chapter 2 describes the current data set and lepton selection criteria.
2. Chapters 3 and 4 describe Monte Carlo samples, lepton identification efficiencies, and fake rate calculations. They also present yields and data-to-Monte Carlo comparison plots for relevant variables in the base and control regions.
3. Chapter 5 discusses neural networks.
4. Chapter 6 presents the maximum likelihood fit used to extract the WZ cross section.
5. Chapter 7 presents all systematic uncertainties on the analysis.
6. Chapters 8 and 9 summarize the results of the likelihood fit and the measurement.

Good run list	$\mathcal{L}$ (fb^{-1})
EM_NOSI	5.3
EM_CMUP_NOSI	5.2
EM_MU_NOSI_CMXIGNORED	5.1
EM_SI	5.1
EM_CMUP_SI	5.0
EM_MU_SI_CMXIGNORED	4.9

Table 1: Luminosity for each of the good run lists (v31) used in this analysis. These have been scaled by the factor of 1.019.

2 Lepton Selection

2.1 Datasets

The triggers considered in this analysis are the high-p_T lepton triggers:

- ELECTRON_CENTRAL18
- MUON_CMUP18
- MUON_CMX18
- MET_PEM
- MUON_CMP18_PHI_GAP

This analysis uses data through P25. We only include runs in the v31 good run lists shown in Table 1.

2.2 Low-Level Selection

This analysis uses the same extended lepton selection as the $H \rightarrow WW$ analysis described in CDF Note 10086 [1]. Below we briefly summarize the lepton types used in this analysis. Full selection criteria for each lepton type are described in Note 10086 [1]. The most significant recent change to lepton selection is that the TCE "tight central electron" category has been replaced by LBE "likelihood-based electrons."

- LBE uses similar identification criteria to TCE, but instead of hard cuts, they are used as variables in a likelihood function which subsequently must pass a cut. See CDF note 10086 [1] for the definition.
- PHX, CMUP, and CMX are JP standard extended to $E_T > 20$ GeV
- CMIO is divided into two fiducial regions:

- CMIOCES is like the JP standard, but fiducial to the CES
- CMIOPES is like the JP standard, but fiducial to the PES and replaces the hit requirements with the simple hit fraction $> 60\%$ and not track χ^2 cut. In addition, we require the number of SVX hits > 3 and the curvature significance > 12 based on error from the covariance matrix.

- CrkTrk includes all tracks not fiducial to the CES or PES and is the JP standard cuts for CMIO with a conversion veto, but with no calorimeter energy requirements (still calorimeter isolated).

2.3 High-Level Selection

Again we use almost the same high-level selection cuts as in Note 8719 to define a signal region. The cuts are summarized below.

- Cosmic-ray rejection
- Opposite-sign dileptons (e or μ)
- Trigger requirement
- $|\Delta z_0| < 4$ cm
- Dilepton invariant mass $M_{ll} > 16$ GeV/c^2
- $\not\!\!E_T^{spec} > 15$ GeV/c^2 for $e\mu$ category, otherwise $\not\!\!E_T^{spec} > 25$ GeV/c^2

The $\not\!\!E_T^{spec}$ is a combination of traditional $\not\!\!E_T$ and $\Delta\phi(\not\!\!E_T, \text{lepton, jet})$, which is the angle between the direction of the $\not\!\!E_T$ and the nearest lepton or jet. The motivation for this variable is to remove even Drell-Yan events where one lepton or jet has been catastrophically mismeasured. The definition is

$$\not\!\!E_{\text{T spec}} \equiv \begin{cases} \not\!\!E_{\text{T}} & \text{if } \Delta\phi(\not\!\!E_{\text{T}}, \text{lepton, jet}) > \frac{\pi}{2} \\ \not\!\!E_{\text{T}} \sin(\Delta\phi(\not\!\!E_{\text{T}}, \text{lepton, jet})) & \text{if } \Delta\phi(\not\!\!E_{\text{T}}, \text{lepton, jet}) < \frac{\pi}{2} \end{cases} \quad (1)$$

We use jets selected with a cone size of $\Delta R < 0.4$ based on the JetClu algorithm. The latest Level 5 corrections[2] are used to correct the absolute energy scale of the jets, and jets are required to have $|\eta| < 2.5$ and $E_{\text{T}} > 15$ GeV/c.

In this analysis the signal region consists only of events with $\not\!\!E_T > 25$ GeV, though any number of jets is allowed. Because the three-lepton signature is associated with relatively high values of missing energy ($\not\!\!E_T$), A large portion of the $Z\gamma$ and Z+jets backgrounds are directly cut out by a high $\not\!\!E_T$ cut. We also select on the Z-mass itself. To do this, we consider all three possible pairings of the three leptons and determine the dilepton invariant masses. If for at least one of the dilepton masses we

[2]Based upon the `jetCorr17` tag of `JetUser` package

have $m_{ll} \in [76.0, 106.0]$ and that particular pair of leptons has same flavor and opposite charges, then we accept the event. Otherwise, the event is rejected.

From there, discriminating variables in the neural net can exploit a variety of geometric and momentum-based values–as well as trilepton flavor combinations–to distinguish background from signal.

3 Signal and Background Estimates

3.1 Backgrounds

Standard Model backgrounds include anything which produces trileptons in the final state with an appreciable cross section times branching ratio. Additional backgrounds come from any source which contains two real leptons and another jet-like object which may "fake" a lepton signature and hence pass the full lepton selection. The latter of these two predominantly come from $Z\gamma$ and Z+jets where the photon or jet fakes a lepton. The Standard Model backgrounds which have true trileptons in the final state considered in this analysis are ZZ and $t\bar{t}$. Each of these backgrounds are described in detail in Note 10020 [2].

- ZZ : PYTHIA is used to simulate this diboson backgrounds. The cross section is relatively small in comparison to the WZ cross section and since four-lepton events are rejected from this analysis the background is composed of only those $ZZ \to llll$ events for which one lepton is not detected. What remains, however, will be the most difficult background to discriminate against.

- $Z\gamma$: The BAUR Monte Carlo program is used to simulate $Z\gamma$ events. These events will be present in the signal sample when the photon is misidentified as a electron.

- Z+jet : These events enter the signal sample when a jet is misidentified as a lepton. This contribution is estimated using fake probabilities calculated from the jet trigger data samples which are applied to events containing one real lepton and one "fakeable object." The estimate of this background is beyond the scope of this note, but it is detailed in the dedicated note CDF Note 10086 [1].

- $t\bar{t}$: PYTHIA is used to simulate these events at $M_t = 175$ GeV/c^2. It is expected that dilepton events from $t\bar{t}$ will have 2 jets (from the b quarks in the decay $t \to Wb$). The contribution of this background is arguably insignificant compared to the WZ, but is still included. Also, it's predilection for two-jets events allows easy discrimination.

  The $t\bar{t}$ process is the smallest background, but arguably the most complex to deal with accurately. This process decays to two pairs of a b-jet accompanied by a W boson. For the case of trileptons, we consider the case of the two W's decaying leptonically. The third lepton signature is then due to one of the b-jets, which is supposed to produce a lepton candidate with higher probability than a light jet, but this rate is not precisely known.

  Because of this, we cannot ignore the possible contribution of $t\bar{t}$ in our data-based Z+jets ("Fakes") background category where a lepton decayed from a b-jet is the fake lepton (denominator object). However, any $t\bar{t}$ that might be included in the high p_T lepton data of the Fakes background is then scaled down by a fake

mode	Period	Stntuple	$\sigma \times \mathcal{B}$ (pb)	K-factor[a]	Filter Eff
WZ	0-23	we0s6d,we0scd,we0shd we0sld,we0sod,we0sbf we0shf	3.46×0.101	1.0	0.754
ZZ	0-23	we0s7d,we0sdd,we0sid we0smd, we0spd,we0scf we0sif	1.511	1.0	0.233
$t\bar{t}$	0-11	te0s2z	7.9×0.1027	1.0	1.0
$Z\gamma$	0-11	re0s33, re0s34, re0s37	14.05	1.36[b]	1.0

[a] If cross section is NLO, then K-factor is one.
[b] http://www-cdf.fnal.gov/tiki/tiki-index.php?page=EwkDatasets#_Drell_Yan_Z_gamma_Sample

Table 2: Monte Carlo samples used in this analysis

rate determined for a sample of jets assumed to be mostly light–hence, the $t\bar{t}$ contribution to the Z+jets ("Fakes") background is scaled down further than it should be since it's jets are the heavy b-jets.

The standard MC $t\bar{t}$ ntuple used by the $H \to WW$ group requires reconstructed leptons to pass a matching criteria to either a generator-level lepton or photon (for the case of photon conversion). For our purposes in the WZ trilepton analysis, we are interested in a third lepton whose signature is the result of those b-jets, so we have our own MC $t\bar{t}$ sample that allows matching to b-jets as well as leptons and photons. The MC $t\bar{t}$ sample accounts for such events that result in three fully identified leptons, as opposed to the 2 leptons+1 fake lepton signature of the Z+jets ("Fakes") background.

Lastly, there is inevitably some overlap between the $t\bar{t}$ that occurs implicitly in the Z+jets ("Fakes") data-based background and the MC sample. By measuring the difference between the 3-lepton bin of the default $t\bar{t}$ sample (lepton match only to generator-level leptons or photons) with another $t\bar{t}$ sample allowing matching to b-jets as well, we take half the percentage difference to be the systematic error (23%) accounting for overlap.

Details on the Monte Carlo samples are shown in Table 2. Background estimates can be found in Table 3.

3.2 WZ Signal

The signal of interest in this analysis is WZ production. Events are simulated with the PYTHIA program. The WZ samples are generated with W inclusive decay and Z leptonic decay (electrons, muons, or taus). The theoretical cross section used is 3.46 ± 0.21, which is an updated prediction from the value used in previous CDF and

Process	Events
ZZ	4.42 ± 0.58
Z+jets	2.82 ± 0.69
Z/γ^*	0.65 ± 0.23
$t\bar{t}$	0.04 ± 0.01
Total Background	7.93 ± 0.96
WZ	35.9 ± 3.63
Signal+Background	43.9 ± 4.10
Data	**48**

Table 3: Expected signal (WZ) and background events. The integrated luminosity is 5.3 fb^{-1}. Errors shown are systematic uncertainties only.

D0 studies (see appendix B). See table 3 for the event counts of background, WZ signal, and data in this analysis.

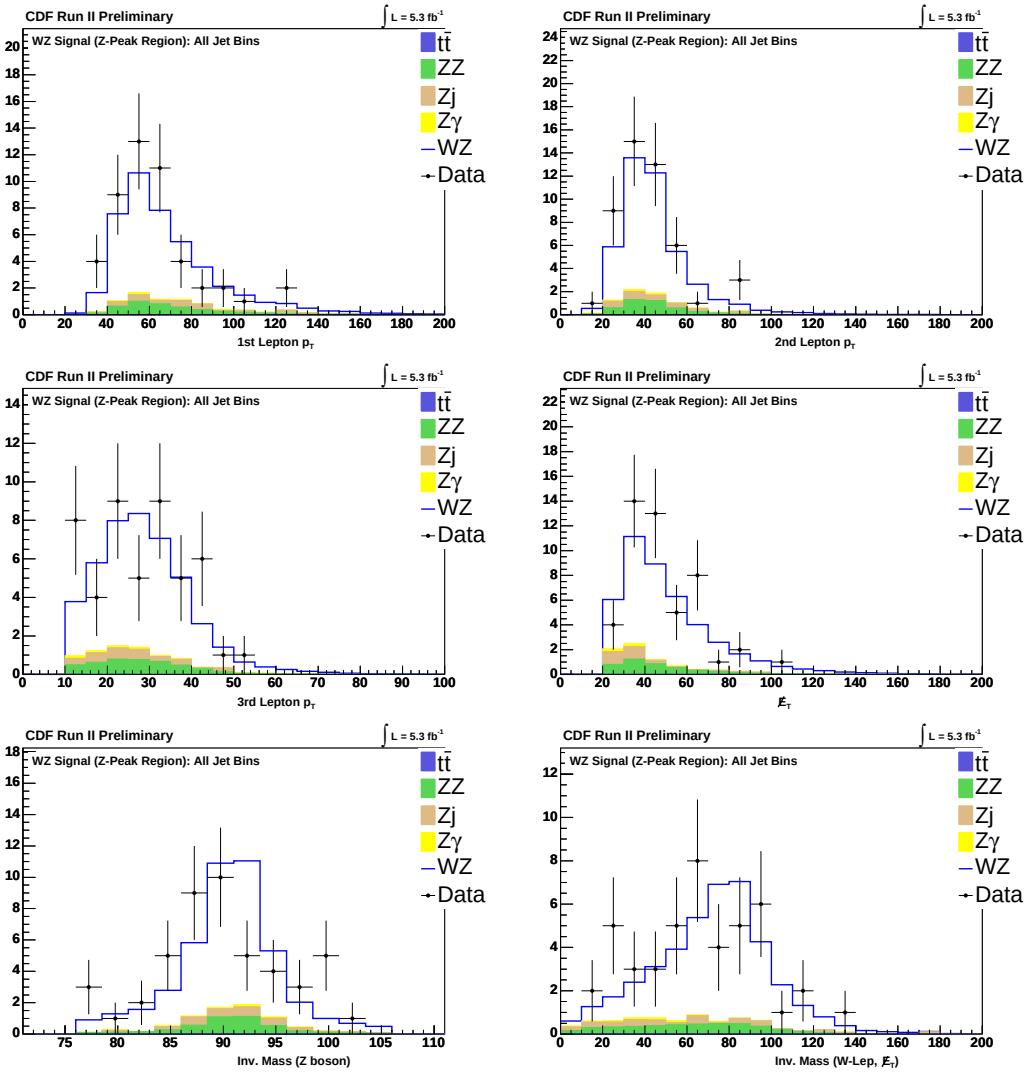

Figure 1: Basic kinematic values of the signal region: Transverse momenta of the three leptons, missing transverse energy ($\not\!\!E_T$) due largely to the neutrino from W's leptonic decay, the reconstructed Z-boson mass, the reconstructed W boson mass.

4 Signal and Control Regions

4.1 Signal Region

The signal region has already been described in Sec. 2.3. Table 3 shows the breakdown of predicted events for signal and backgrounds and Figure 1 shows comparisons between the data and predicted events for several kinematic variables. The plots and table reproduced here are representative of the good agreement between data and predicted events in the signal region.

Process	Events		
ZZ	3.15	$\pm$	0.42
Z+jets	14.7	$\pm$	3.60
Z/γ^*	12.8	$\pm$	4.47
$t\bar{t}$	0.004	$\pm$	0.001
Total Background	30.6	$\pm$	5.82
WZ	4.43	$\pm$	0.45
Signal+Background	35.0	$\pm$	6.00
Data	**36**		

Table 4: Low $\not{E}_T$ Control Region

4.2 Control Regions

Two control regions, orthogonal to both each other and the signal region, have been selected to test background modeling against the data. Each are described below and agree well with data.

Low $\not{E}_T$ Region

Recall that the signal region establishes a $\not{E}_T > 25.0$ cut to remove most of the $Z\gamma$ and Z+Jets background. Because of the leptonic decay of the W in the WZ trilepton signal, it has an inherently high missing transverse energy distribution and the $\not{E}_T > 25.0$ removes little signal. As such, the first control region is a low $\not{E}_T$ region ($10.0 < \not{E}_T < 20.0$ GeV) where the Z lepton pair is selected for with the same criteria as the signal region. The event count for the low $\not{E}_T$ control region is in table 4 and basic values are plotted in figure 2.

Z Peak Removed Region

The second control region selects against the Z lepton pair with a wide window around the Z mass. That is, any event with at least one of its three dilepton pairings having $m_{ll} \in [66.0, 116.0]$ GeV, with same flavor and opposite charge, is selected *against*. Note that the signal region selects events showing a Z mass within ± 15 GeV of 91.0 GeV, whereas this control region selects against events showing a Z mass within ± 25 GeV of 91.0 GeV. The event count for the Z-peak removed control region is in table 5 and basic distributions are in figure 3.

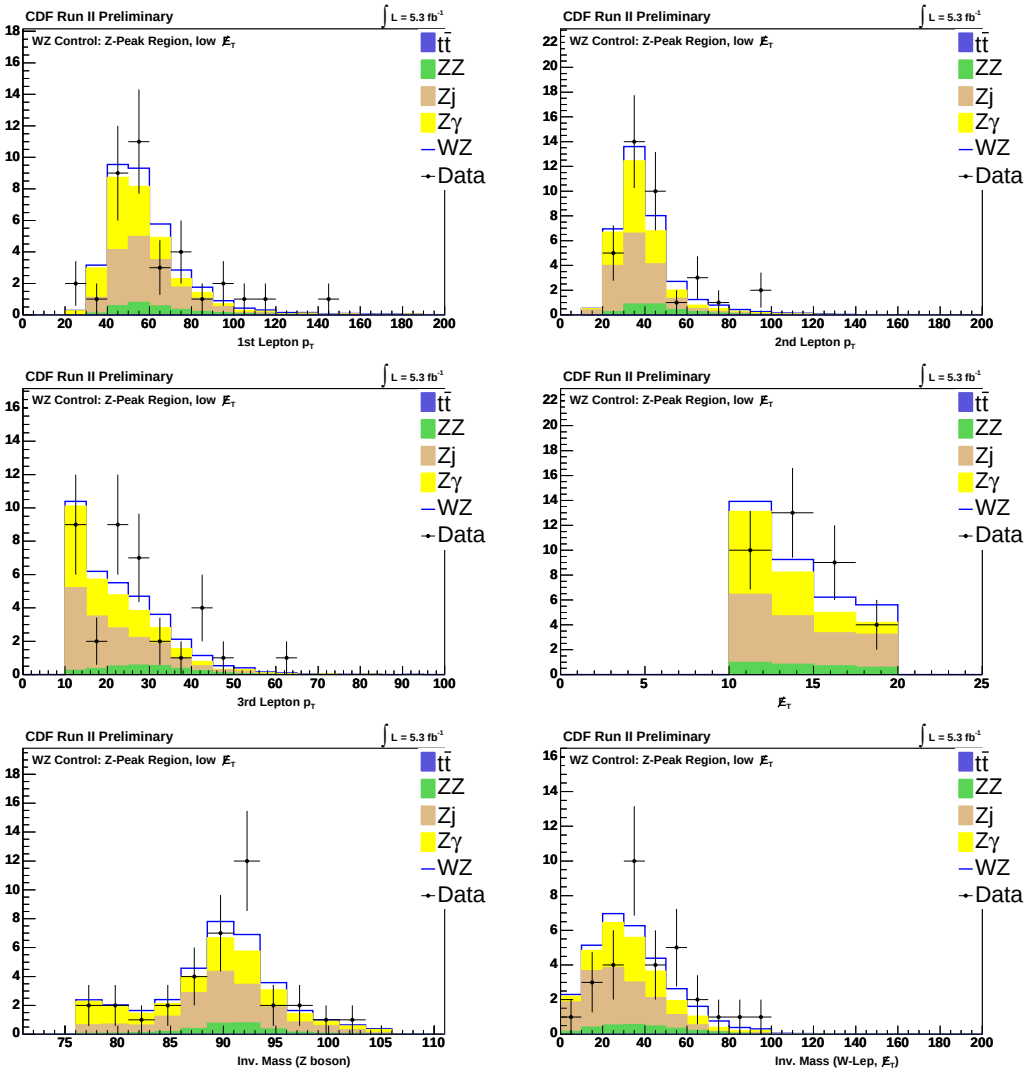

Figure 2: Low $\not\!\!E_T$ Region: Transverse momenta of the three leptons, missing transverse energy ($\not\!\!E_T$) due largely to the neutrino from W's leptonic decay, the reconstructed Z-boson mass, the reconstructed W boson mass.

Process	Events
ZZ	1.16 ± 0.15
Z+jets	6.49 ± 1.59
Z/γ^*	15.5 ± 5.44
$t\bar{t}$	0.14 ± 0.04
Total Background	23.3 ± 5.71
WZ	3.04 ± 0.31
Signal+Background	26.3 ± 5.85
Data	**23**

Table 5: Z Peak Removed Region

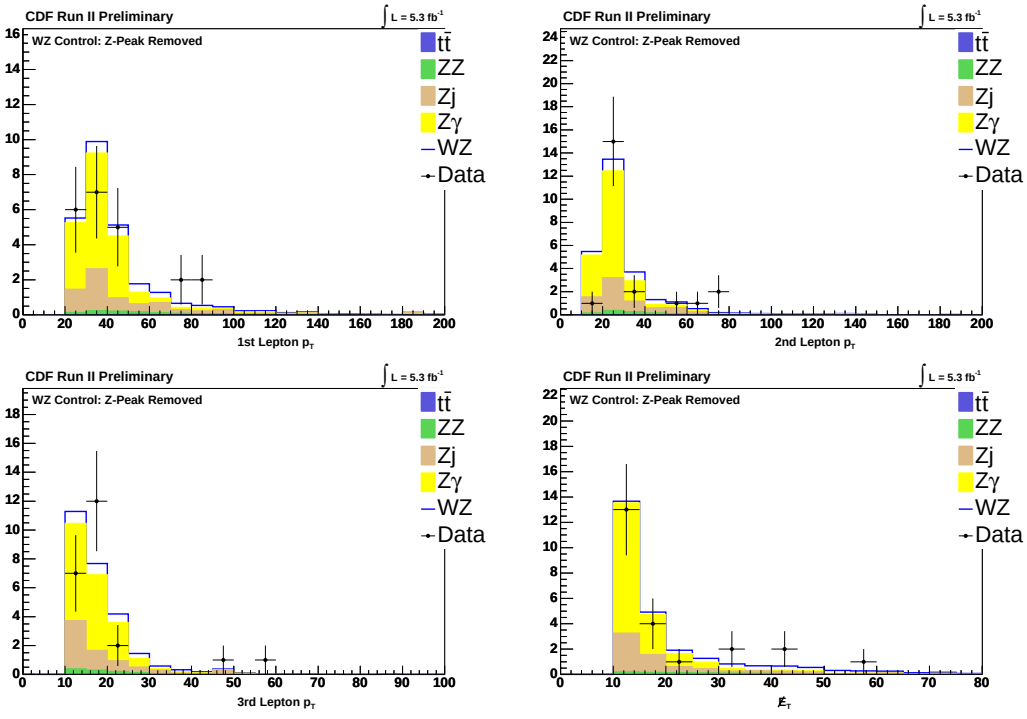

Figure 3:

5 Neural Network

The trilepton WZ analysis relies on the NeuroBayes neural network package to discriminate signal from background; we do not attempt the Matrix Element method in this study. We use 12 input variables. The neural net results can be seen in figure 4.

Because the interaction topology under consideration involves three leptons and also because we do not separate the analyses by jet bin, the signatures of the signal region under consideration involve many potentially complex variables whose discriminatory power must be explored. As such, a large quantity of discriminating variables are used to train the NeuroBayes neural nets.

The discriminating variables are, in order of significance:

1. $\Delta\phi$ (W-Lep., $\not\!\!E_T$) (see figure 5)
2. m_T (jets), 0-jet events just assigned a value of zero. (see figure 5)
3. Lepton type combinations: discriminate by whether an event is eee (three electrons), $ee\mu$, $e\mu\mu$, etc. This variable is particularly good at discriminating $Z\gamma$ because of the photon conversion to electrons. For instance, eee is strong in $Z\gamma$, but $ee\mu$ is not because the same-flavor pair ee would be from the Z which means the μ would have to be from the conversion. However, photon conversion tends to be to electrons, not to muons. (see figure 5)
4. $\not\!\!E_T$ (see figure 6)
5. m_T (W-Lep., $\not\!\!E_T$) (see figure 6)
6. $\Delta\phi$ (2^{nd} Lep., $\not\!\!E_T$) (see figure 6)
7. H_T (see figure 7)
8. m_T (3^{rd} Lep., $\not\!\!E_T$, Jets) (see figure 7)
9. m_T (3^{rd} Lep., $\not\!\!E_T$) (see figure 7)
10. $\Delta\phi$ (vector sum of the three leptons, $\not\!\!E_T$) (see figure 8)
11. m_T (three leptons) (see figure 8)
12. NJet (see figure 8)

See appendix A for histograms of the discriminating variables in the control regions.

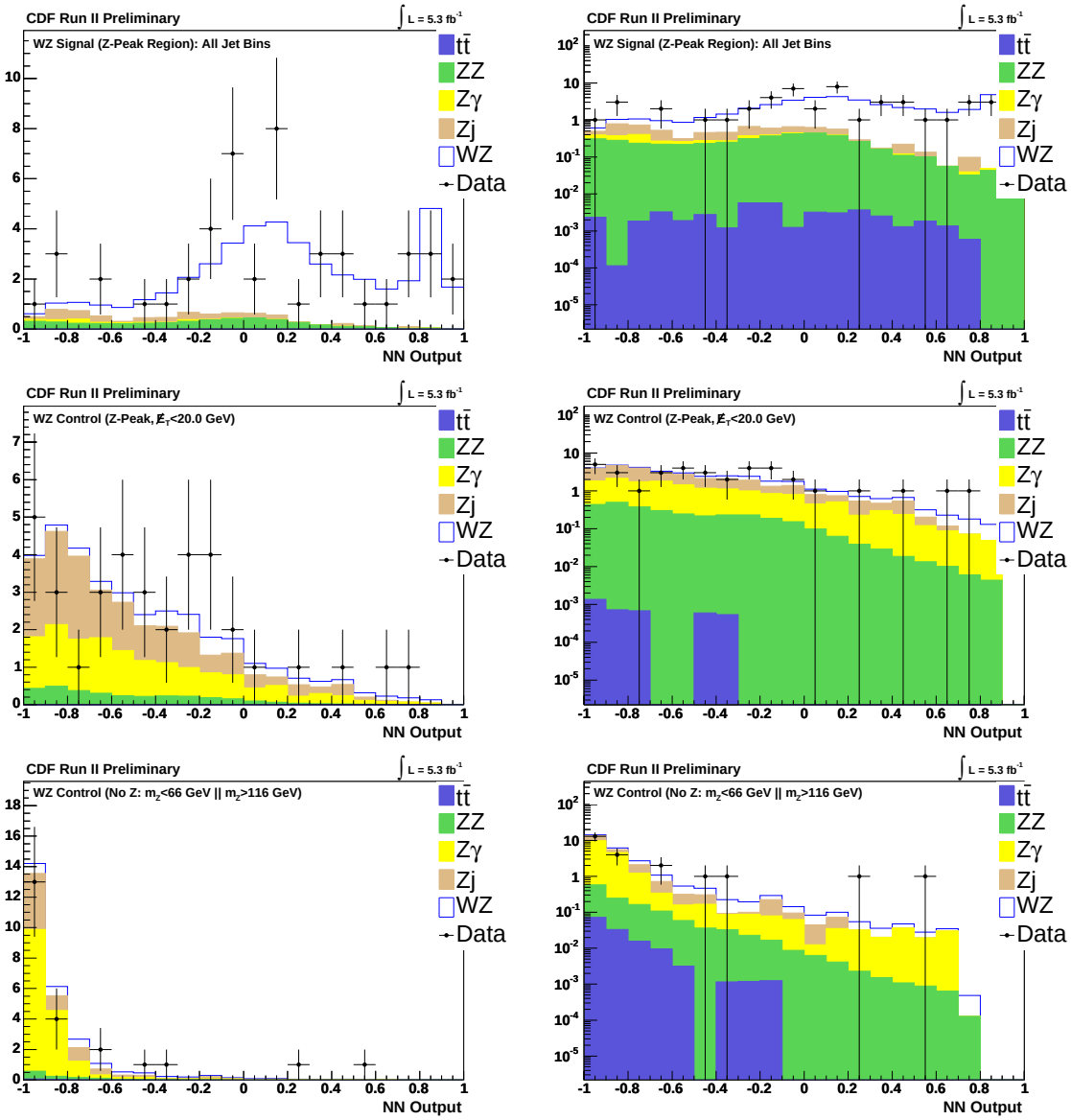

Figure 4: Trilepton WZ NeuroBayes Neural Network output. Top two: signal region. Middle two: low $\not\!\!E_T$ control region. Bottom two: Z-Peak removed control region.

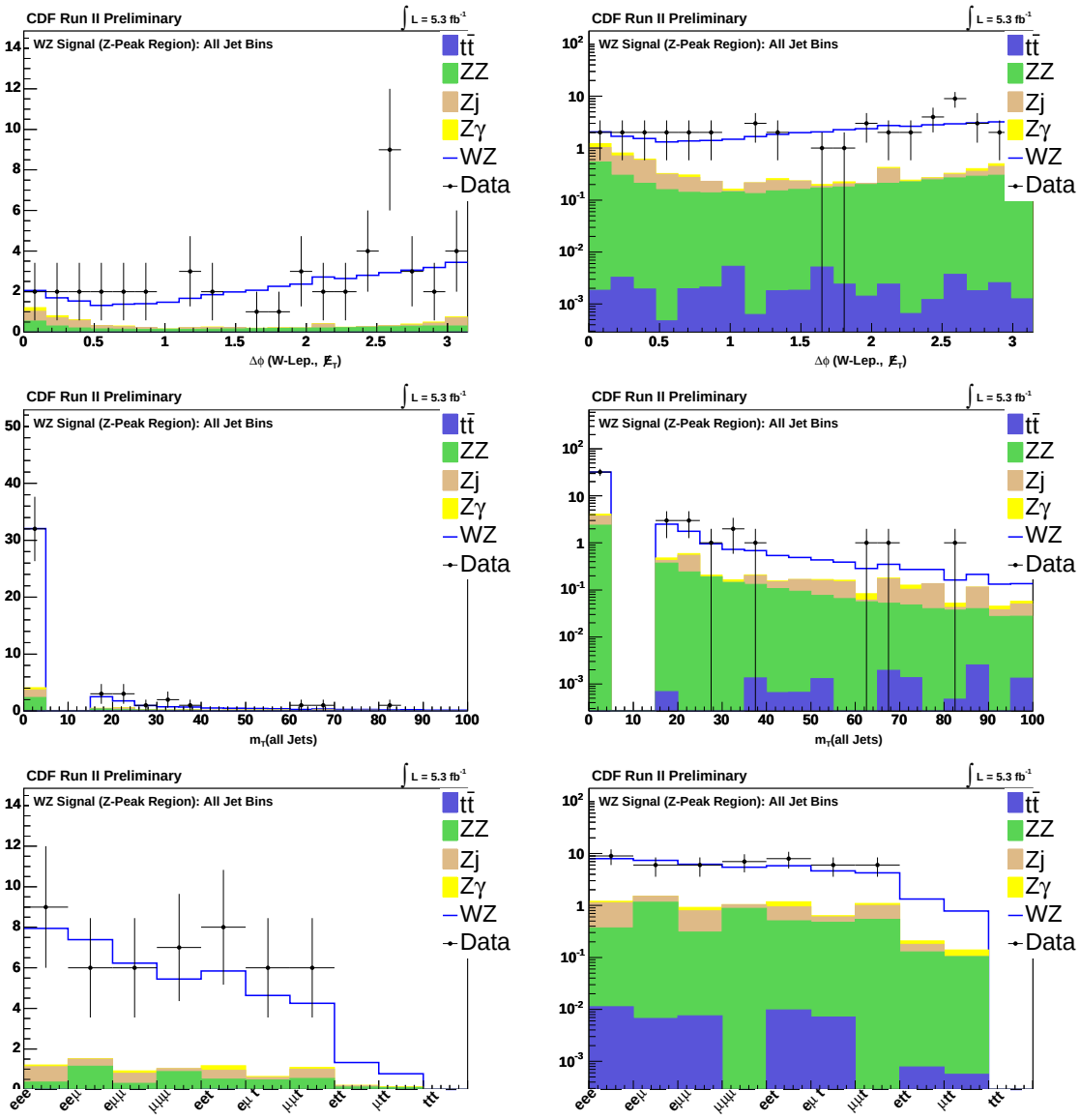

Figure 5: $\Delta\phi$ (W-Lep., $\not\!\!E_T$), m_T (jets), lepton flavor combination

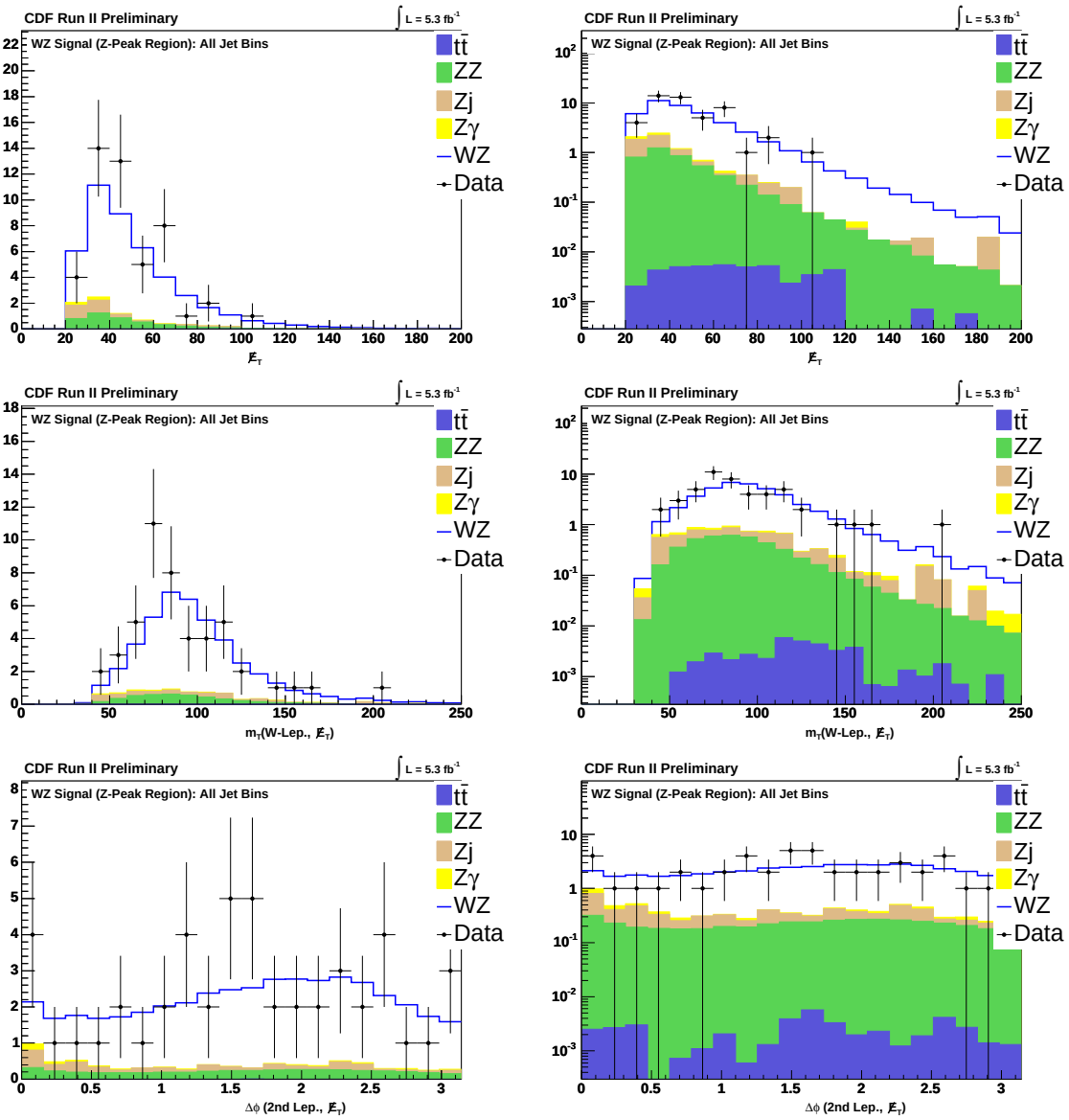

Figure 6: $\not\!\!E_T$, m_T (W-Lep., $\not\!\!E_T$), $\Delta\phi$ (2^{nd} Lep., $\not\!\!E_T$)

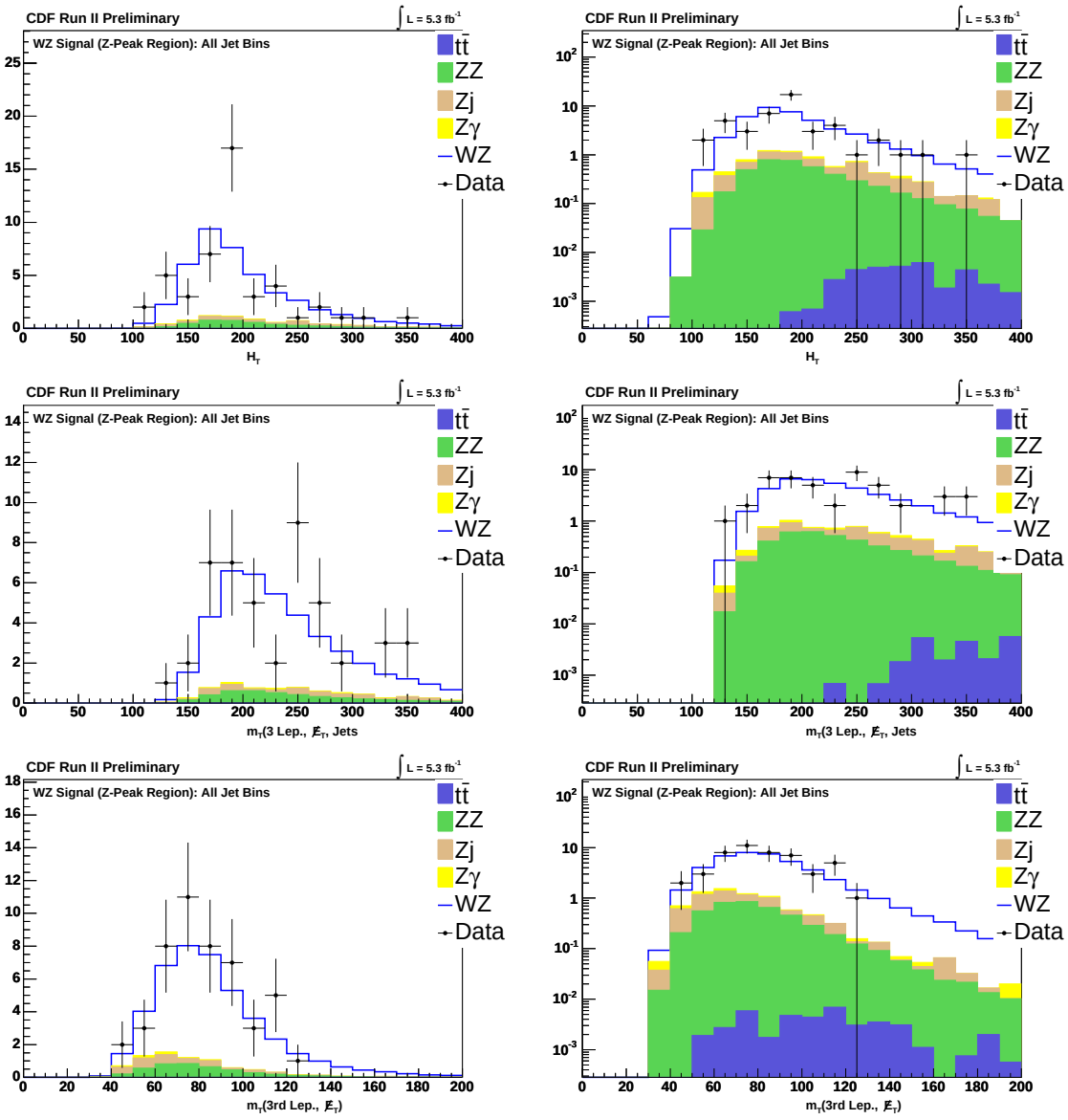

Figure 7: H_T, m_T (3$^{\text{rd}}$ Lep., $\not\!\!E_T$, Jets), m_T (3$^{\text{rd}}$ Lep., $\not\!\!E_T$)

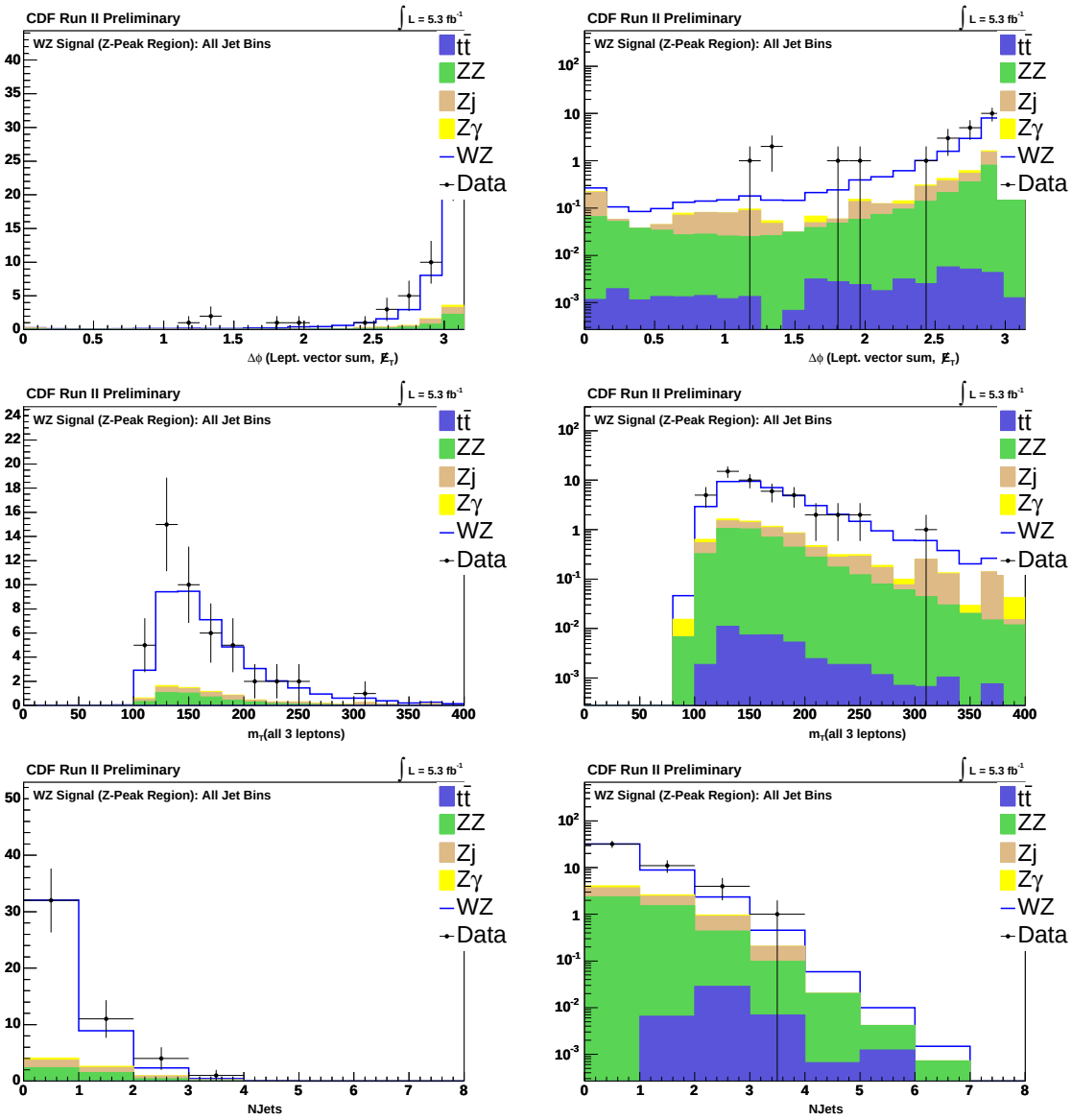

Figure 8: $\Delta\phi$ (vector sum of the three leptons, $\not\!\!E_T$), m_T (three leptons), NJet

6 Maximum Likelihood Method

A binned maximum likelihood method is used to extract the WZ cross section using the shape of the LR_{WZ} distributions from signal and background along with their estimated normalizations and systematic uncertainties. The best fit to these distributions, or the maximum likelihood, gives the best measure of the WZ cross section.

The likelihood function is formed from a product of Poisson probabilities for each bin in LR_{WZ}. Additionally, Gaussian constraints are applied corresponding to each systematic S_c (shown in Table 6). The likelihood is given by

$$\mathcal{L} = \left(\prod_i \frac{\mu_i^{n_i} e^{-\mu_i}}{n_i!} \right) \cdot \prod_c e^{\frac{S_c^2}{2}} \tag{2}$$

where μ_i is the total expectation in the i-th bin and n_i is the number of data events in the i-th bin. μ_i is given by

$$\mu_i = \sum_k \alpha_k \left[\prod_c (1 + f_k^c S_c) \right] (N_k^{Exp})_i \tag{3}$$

Here f_k^c is the fractional uncertainty associated with the systematic S_c and process k. This is constructed such that the systematics are properly correlated (or uncorrelated) between the different contributions[3]. $(N_k^{Exp})_i$ is the expected number of events from process k in the i-th bin. α_k is the parameter which is used to measure the WZ cross section. It is a freely floating parameter for α_{WZ} and fixed for all other processes. In this sense it allows one to measure an additional overall normalization factor for the WZ process. The measured value of this parameter (α_{WZ}) multiplied by the input WZ cross section gives the measured value of the WZ cross section, or if you like:

$$\sigma_{WZ}^{measured} = \alpha_{WZ} \cdot \sigma_{WZ}^{NLO}$$

In practice it is the negative log likelihood which is minimized, which is equivalent to maximizing the likelihood. The MINUIT program is used to minimize this function and MINOS is used to extract the error on this minimization. The asymmetric errors from MINOS are the errors used in this analysis.

6.1 Pseudo-experiments

In order to quantify our expectations 10,000 pseudo-experiments are generated, each of which is treated exactly as data would be in the minimization. In generating pseudo-experiments, care has been taken to ensure that variations of the systematic parameters (S_c) are correctly correlated (or uncorrelated) between processes. This is done in the following way:

[3]Note that if a systematic is partially correlated it is possible to decompose that into its correlated and uncorrelated parts

- Construct an array of Gaussianly distributed numbers g_c
- Fluctuate the nominal prediction (N_k^{Exp}) for each process k according to their fractional uncertainties (f_k^c) and the systematic fluctuations (g_c) such that the new "Gaussianly" fluctuated number is

$$G_k = N_k^{Exp} \prod_c (1 + f_k^c g_c).$$

- Poisson fluctuate the resulting number:

$$P_k = \text{Poisson}(G_k).$$

P_k is then the number of events which will be drawn at random from process k (the LR_{WZ} template for process k) with a probability according to its distribution. Fig. 9 summarize the results of these pseudo-experiments for the only floating parameter, α_{WZ}. Results for the constrained parameters are shown in App. C.

The pull for asymmetric errors is defined as

$$g = \begin{cases} \frac{\tau_g - \tau_m}{|\sigma_m^+|} & \text{for } \tau_m \leq \tau_g \\ \frac{\tau_m - \tau_g}{|\sigma_m^-|} & \text{for } \tau_m > \tau_g \end{cases} \tag{4}$$

where τ_g is the generated value and τ_m is the measured value, and $\sigma_m^{\pm}$ are the positive and negative errors. While the pull distribution for α_{WZ} appears to be generally Gaussian, note that for asymmetric errors this is not guaranteed to be the case [7]. The mean of the Gaussian fit to the pull distribution is displaced from zero by 0.062, which could indicate a fit bias on the value of α_{WZ}. To check for fit bias, we plot the distribution of differences, $\tau_g - \tau_m$, and fit it to a Gaussian as shown in Fig. 10 as 0.0007 ± 0.002. The mean of this Gaussian gives the fit bias, but compared to the fit value of 1.052 this bias is completely negligible.

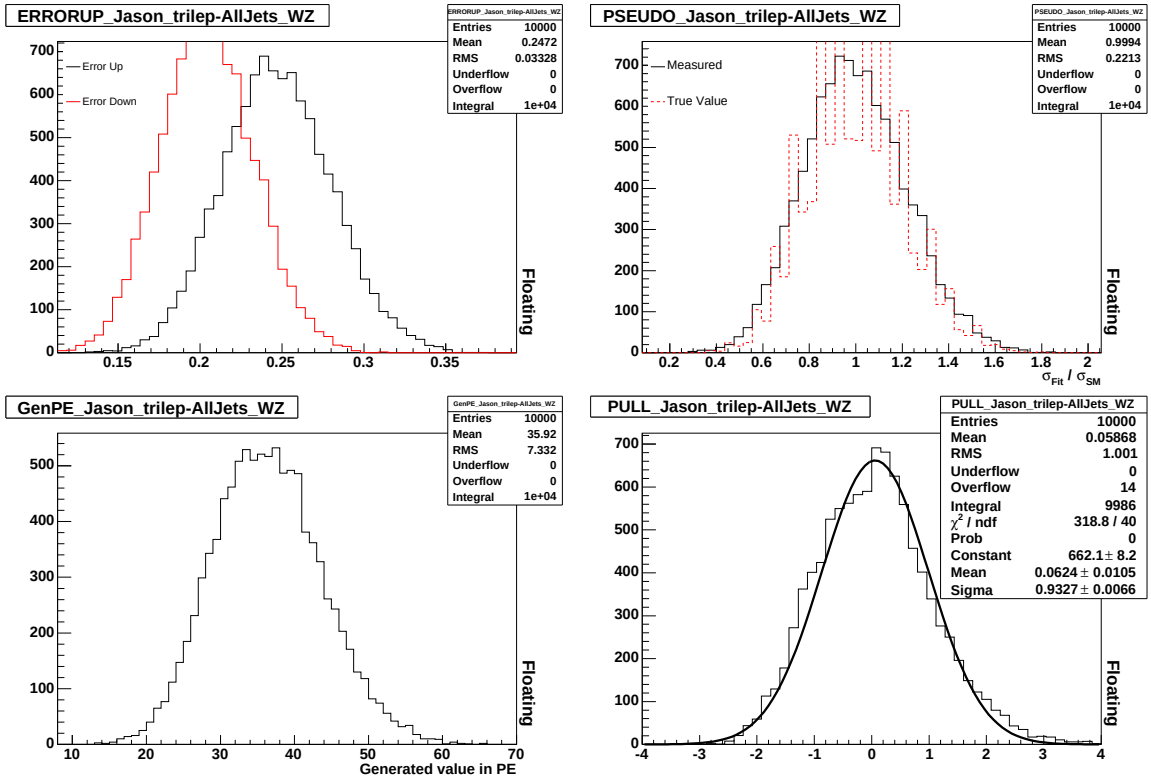

Figure 9: Generated and measured values for α_{WZ} from 10k pseudo-experiments. From the top left clockwise: the measured positive and negative errors, the measured and generated values of α_{WZ}, the number of WZ events in each pseudo-experiment, and the pull distribution for α_{WZ}. The "generated value of α_{WZ}" is a loose term which really means P_{WZ}/N_{WZ}^{Exp}.

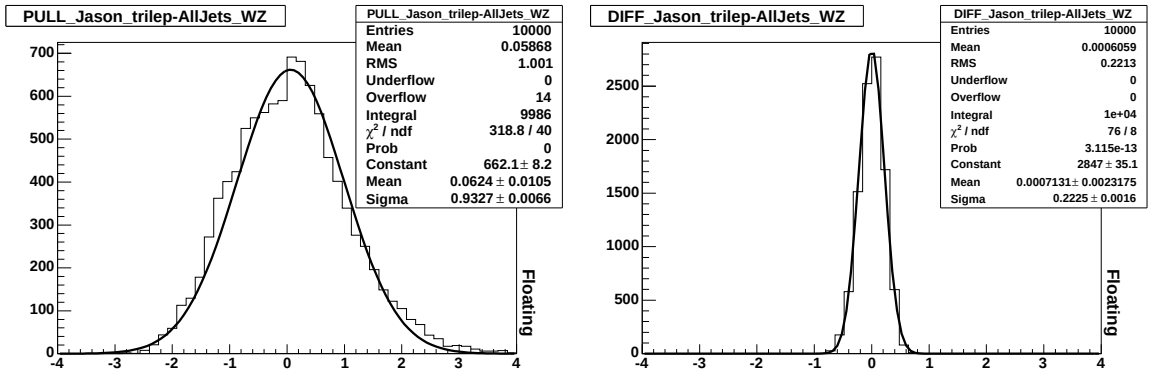

Figure 10: Generated and measured values for α_{WZ} from 10k pseudo-experiments. The plot on the left shows the pull distribution for α_{WZ} while the plot on the right shows the difference distribution for α_{WZ}. Although the pull distribution shows some displacement from a mean of zero, the difference distribution shows the actual fit bias is negligibly small.

7 Systematic Uncertainties

All of the systematics used in this analysis are briefly described here. This analysis uses exactly the same lepton and event selection as the $H \rightarrow WW$ trilepton analysis and thus the systematics used are the same as those in the $H \rightarrow WW$ trilepton analysis. For more details on how these systematic uncertainties were derived please see CDF Notes 8719 [4] and 9685 [3].

The systematics are summarized in table 6.

- **Conv** : This systematic refers to the uncertainty in the photon conversion removal efficiency. It is only applied to $Z\gamma$ events, where a significant photon conversion background is expected. This systematic has been estimated at 20% as can be found in CDF Note 8073 [6].

- **DibоAcc** : This systematic refers to the uncertainty on the acceptance of events from diboson processes (WZ and ZZ). Since the production processes are very similar, we assume these uncertainties are correlated.

- **ttAcc** : This systematic refers to the uncertainty on the acceptance of events from $t\bar{t}$, which is uncorrelated from other acceptance uncertainties. At leading order, $t\bar{t}$ has two W-bosons that decay leptonically to provide two leptons, with the third lepton faked from one of the two b-jets for the event to be in the signal region.

- **PDF** : This uncertainty is calculated in the usual manner by looking at the maximum and minimum difference using the CTEQ6m eigenvectors and weighting the acceptance. These uncertainties range from 1.9 to 4.1%.

- **ID** : The estimated errors in lepton identification efficiencies are fluctuated up and down by 1σ. The difference in acceptance of these two fluctuations divided by the nominal acceptance is taken to be the uncertainty due to varying the lepton identification efficiency. All lepton efficiencies are varied in the same direction simultaneously.

- **Trig** : The trigger efficiencies are varied up and down by their 1σ uncertainties to determine the % change in the acceptance, which is taken to be the systematic quoted here. The trigger efficiencies are varied in a correlated way.

- **Fake** : Fake probabilities, or the probability that a jet-like object will be falsely identified as a lepton, are calculated using the jet-triggered data samples. These fake probabilities are calculated as a function of both lepton type and E_T (or p_T). These probabiities are then applied to the Z+jets (fakeable object) sample from data. The fake probabilities are varied up and down to get an estimate of the uncertainty on the yield. This systematic only applies to the fakes (or Z+jets) sample.

- **Lumi** : The standard 5.9% uncertainty is taken on the luminosity. The exception to this is the Z+jets sample, which we do not assign a luminosity uncertainty since it is derived from the data itself.

- **MCDep** : Some of the Monte Carlo samples used in this analysis do not span the entire run range used, as shown in Table 2. For this reason a systematic uncertainty is assigned based on the acceptance difference of a sample which does span the entire run range. Only $Z\gamma$ requires the MCDep systematic in this analysis.

- **XSDibo, XStt, and XSZg** : These uncertainties refer to the theoretical uncertainties on the cross sections used in this analysis. Because we are measuring the WZ cross section, we do not assign it a systematic uncertainty.

- **b-jet Fake** Although $t\bar{t}$ is a small contribution to the background for the WZ cross section in the trilepton case, we do have to account for the peculiar situation that our third lepton is faked from a b-jet and the rate at which a b-jet fakes a lepton–as opposed to a light jet–is not well-known. Further, as a background with two real leptons and one faked, we cannot ignore the possible coverage of $t\bar{t}$ in the data-based Fakes (Z+Jets) category. We know that the fake rates used in the Fakes category is based on jet samples populated mostly with light jets and presume that b-jets in particular are more likely than light jets to produce a signature that could fake a lepton. Hence, whatever $t\bar{t}$ contribution that exists in the Fakes category is scaled down by the light jet dominated fake rate, meaning it is scaled down too far. To make up for the difference we use an MC $t\bar{t}$ sample that allows reconstructed leptons to match to generator-level leptons, photons, or b-jets (typically, for these reconstructed MC leptons to be considered fully "found" they must pass a matching criterion to a generator-level lepton or photon only). Now, of course, we have the problem of possible double-counting of $t\bar{t}$ between the MC and what implicit $t\bar{t}$ contribution populates the Fakes category. To account for the double-counting possibility, we assign a systematic error defined to be one half the percentage difference between the MC $t\bar{t}$ sample that allows leptons to match to generator-level leptons, photons, and b-jets; and the MC $t\bar{t}$ sample that allows such matching to generator-level leptons and photons only.

Systematic Uncertainty	WZ	ZZ	$Z\gamma$	$t\bar{t}$	Fakes
Diboson Acceptance	0.100	0.100			
$t\bar{t}$ Higher Order Diagrams				0.100	
PDF Model	0.027	0.027		0.021	
Lepton ID Efficiencies	0.020	0.020		0.020	
Trigger Efficiences	0.021	0.021		0.020	
Light Jet Fake Rates					0.245*
b-Jet Fake Rate*				0.23	
Luminosity	0.059	0.059		0.059	
MC Run Dependence			0.050		
Jet Energy Scale			0.012*		
$Z\gamma$ Higher Order Diagrams*			0.110		
$Z\gamma$ Conversion			0.20†		
σ_{Diboson}		0.060			
$\sigma_{t\bar{t}}$				0.100	
$\sigma_{\text{Z}\gamma}$*			0.050		

Table 6:

* New to WZ analysis.
† Replaces the '$W\gamma$ scale' systematic, $Z\gamma$ no longer scaled down.

Parameter	Fitted value	Positive Error	Negative Error
α_{WZ}	1.0499986	0.2564867	0.2126791
ZγConv	0.0167314	0.9991208	0.9991019
DiboAcc	0.0706744	0.9970620	0.9971993
ttAcc	0.0000892	0.9970620	0.9999997
PDF	0.0226481	0.9995643	0.9995942
ID	0.0158314	0.9998039	0.9998275
Trig	0.0177994	0.9997231	0.9997469
Fake	0.2134870	0.9833000	0.9818139
Lumi	0.0468501	0.9983436	0.9984017
MCDep	0.0041960	0.9999441	0.9999442
XSDibo	0.0425243	0.9989665	0.9989443
XStt	0.0000892	0.9999997	0.9999997
XSZg	0.0041960	0.9999441	0.9999442
bfake	0.0041960	0.9999441	0.9999442
$Z\gamma$Acc	0.0092238	0.9997312	0.9997287
JES	0.0010072	0.9999967	0.9999968

Table 7: Fit values for all parameters in the fit. α_{WZ} is allowed to float unconstrained while the other parameters (S_c) are constrained in the likelihood each by a unit Gaussian. α_{WZ} is an absolute normalization. Since the constrained parameters S_c are multiplied by the estimated 1σ errors (f_k^c) (see equations 2 and 3) they are given in units of sigma.

8 Results

The fit gives a measured value for the WZ cross section of

$$\sigma(p\bar{p} \to WZ) = 3.63^{+0.89}_{-0.73}(\text{pb}) \tag{5}$$

where the uncertainty includes statistical, systematic, and luminosity uncertainties. Separating out the statistical and systematic uncertainties gives

$$\sigma(p\bar{p} \to WZ) = 3.63^{+0.68}_{-0.61}|_{\text{stat}}{}^{+0.57}_{-0.40}|_{\text{syst}}(\text{pb}) \tag{6}$$

where the systematic uncertainty quoted includes a 5.9% luminosity uncertainty. This corresponds to $\alpha_{WZ} = 1.050^{+0.256}_{-0.213}$. The fitted values for all parameters are shown in Table 7. The fitted templates are shown in Figure 11.

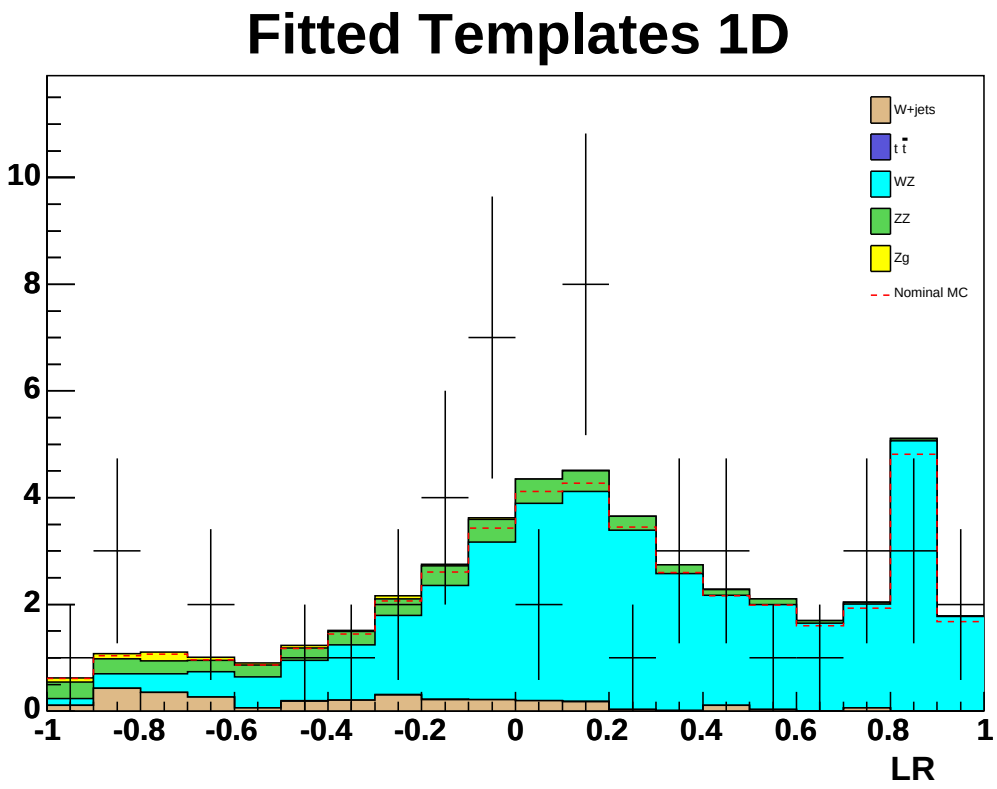

Figure 11: Fitted templates to the data. The nominal prediction including signal and all backgrounds before the fit is given as the red dashed line.

9 Summary

In this analysis we use the same lepton selection used in the $H \rightarrow WW$ group along with neural net based likelihood ratios to extract the WZ production cross section in the trilepton channel. The cross section is measured by creating LR_{WZ} templates for each process using signal and background-like events and then constructing a binned likelihood from Poisson probabilities. Gaussian terms in the likelihood are used to constrain systematics within their estimated uncertainties. The WZ contribution is allowed to float freely and it is this cross section, or normalization, which is the value of interest.

The measured cross section using 5.3 fb^{-1} of data is $\sigma(p\bar{p} \rightarrow WZ) = 3.63^{+0.68}_{-0.61}|_{\rm stat}{}^{+0.57}_{-0.40}|_{\rm syst}$(pb) pb. This is in good agreement with the updated theoretical prediction of $\sigma_{WZ}^{NLO} = 3.46 \pm 0.21$ pb. This is also a substantial improvement over the published CDF analysis, which measured a WZ cross section in the trilepton channel of $5.0^{+1.8}_{-1.4}$(stat) ± 0.4(syst) pb [5].

References

[1] "Benjamin, D and Kruse, M and James, E and Jindariani, S Rutherford, B Lysak, R and Hidas, D and Robson, A and St.Denis, R and Bussey, P and Herndon, M and Nett, J and Pursley, J and d'Errico, M and PaganGriso, S and Lucchesi", *Search for $H \rightarrow WW$ Production Using* 5.3fb^{-1}, (2010), CDF/PHYS/EXOTIC/CDFR/10086. 4, 7

[2] "Benjamin, D and Kruse, M and James, E and Jindariani, S Rutherford, B Lysak, R and Hidas, D and Robson, A and St.Denis, R and Bussey, P and Herndon, M and Nett, J and Pursley, J and d'Errico, M and PaganGriso, S and Lucchesi", *Search for $VH \rightarrow VWW$ SM Higgs Production in the Trilepton Signature*, (2009), CDF/PHYS/EXOTIC/CDFR/10020. 3, 7

[3] "Benjamin, D and Bussey, P and Herndon, M and Hidas, D and James, E and Jindariani, S and Kruse, M and Lucchesi, D and Lysak, R and PaganGriso, S and Robson, A and Rutherford, B and St.Denis, R and Pursley, J", *Search for $H \rightarrow WW$ Production Using 3.6 fb^{-1}*, (2009), CDF/PHYS/EXOTIC/CDFR/9685. 23, 36

[4] "Hsu, S.-C. and Lipeles, E. and McCarthy, K. and Neubauer, M.S. and Wurthwein, F.", *Search for $H \rightarrow WW$ Production with Matrix Element Methods Using 1.1* fb^{-1}, (2007), CDF/PHYS/EXOTIC/CDFR/8719. 23

[5] "Neubauer, Mark and *et al.*" *Observation of WZ Production*, Phys.Rev.Lett.98:161801 (2007), arXiv:hep-ex/0702027v1. 3, 28

[6] "Attal, Alon and Canepa, Anadi", *Photon Conversion Removal Efficiency*, (2006), CDF/ANAL/ELECTRON/CDFR/8073. 23

[7] "Demortier, Luc and Lyons, Louis" *Everything You Always Wanted to Know About Pulls* (2002), CDF/ANAL/PUBLIC/5776. 21

[8] http://www-cdf.fnal.gov/physics/ewk/2007/WZ_2fb/ 3

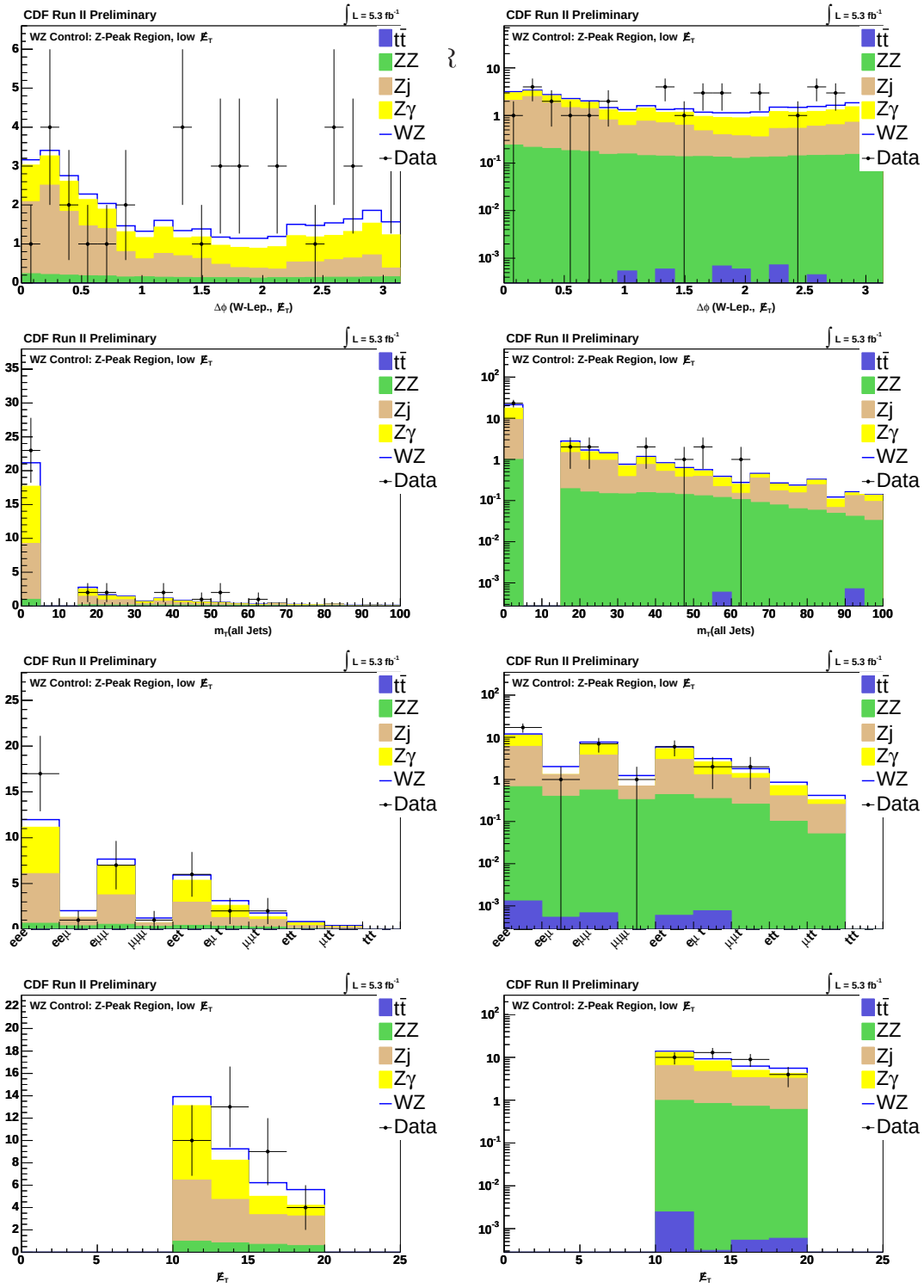

Figure 12: Low $\not\!\!E_T$ Control Region: $\Delta\phi$ (W-Lep., $\not\!\!E_T$), m_T (jets), lepton flavor combination, $\not\!\!E_T$

A WZ Control Region Discriminating Variables

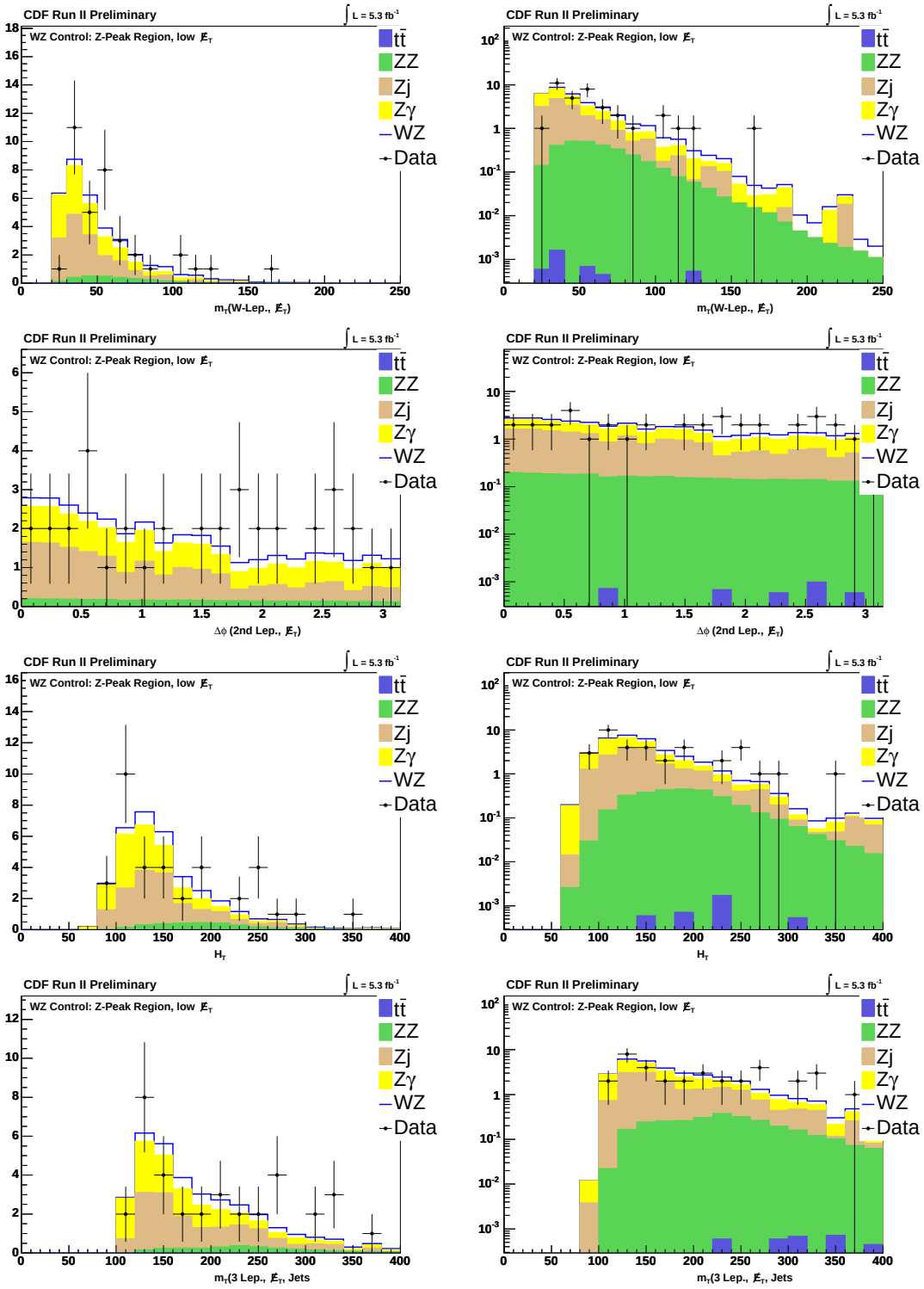

Figure 13: Low $\not\!\!E_T$ Control Region: $\not\!\!E_T$, m_T (W-Lep., $\not\!\!E_T$), $\Delta\phi$ (2^{nd} Lep., $\not\!\!E_T$)

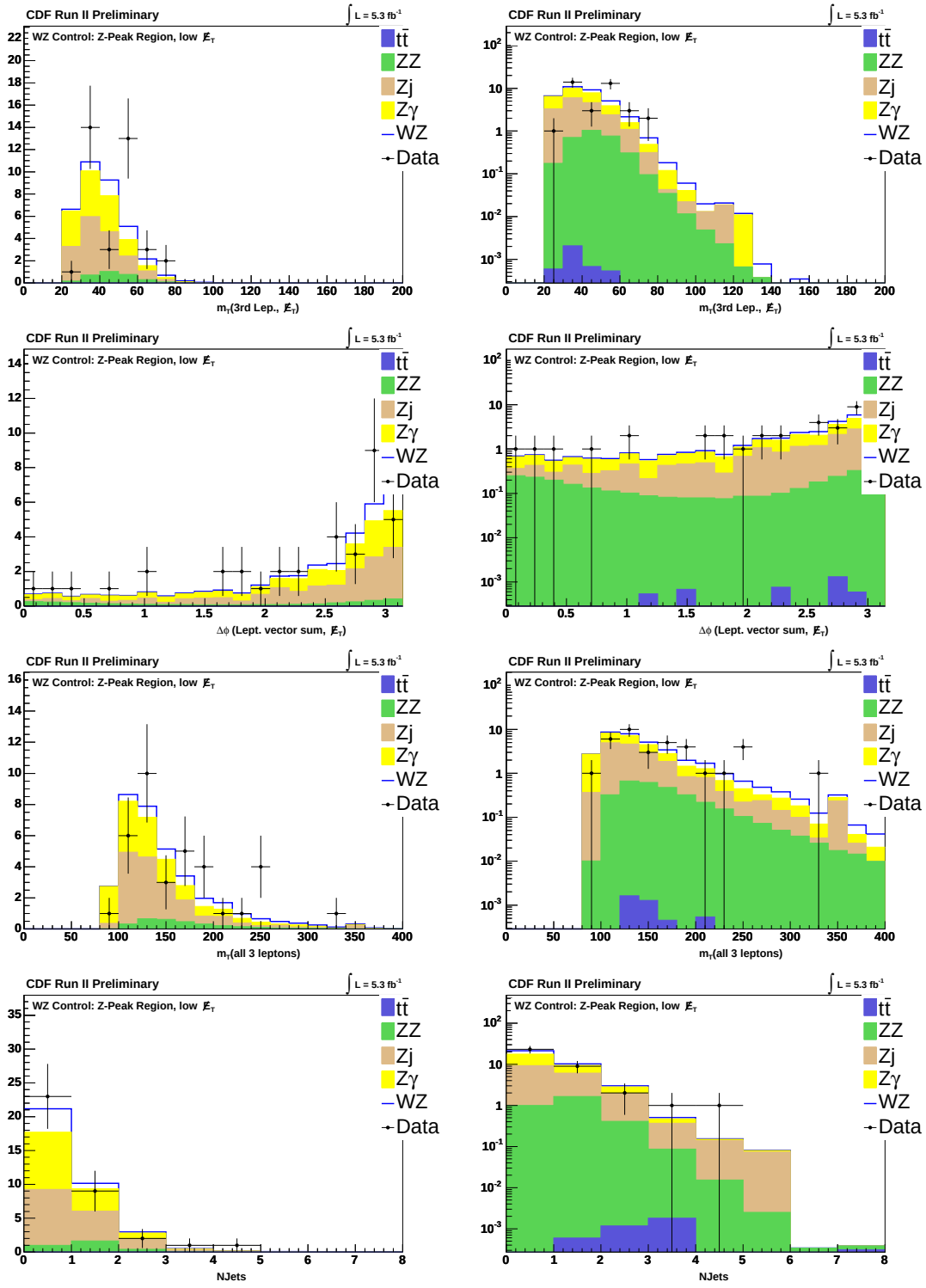

Figure 14: Low $\not\!\!E_T$ Control Region: H_T, m_T (3rd Lep., $\not\!\!E_T$, Jets), m_T (3rd Lep., $\not\!\!E_T$)

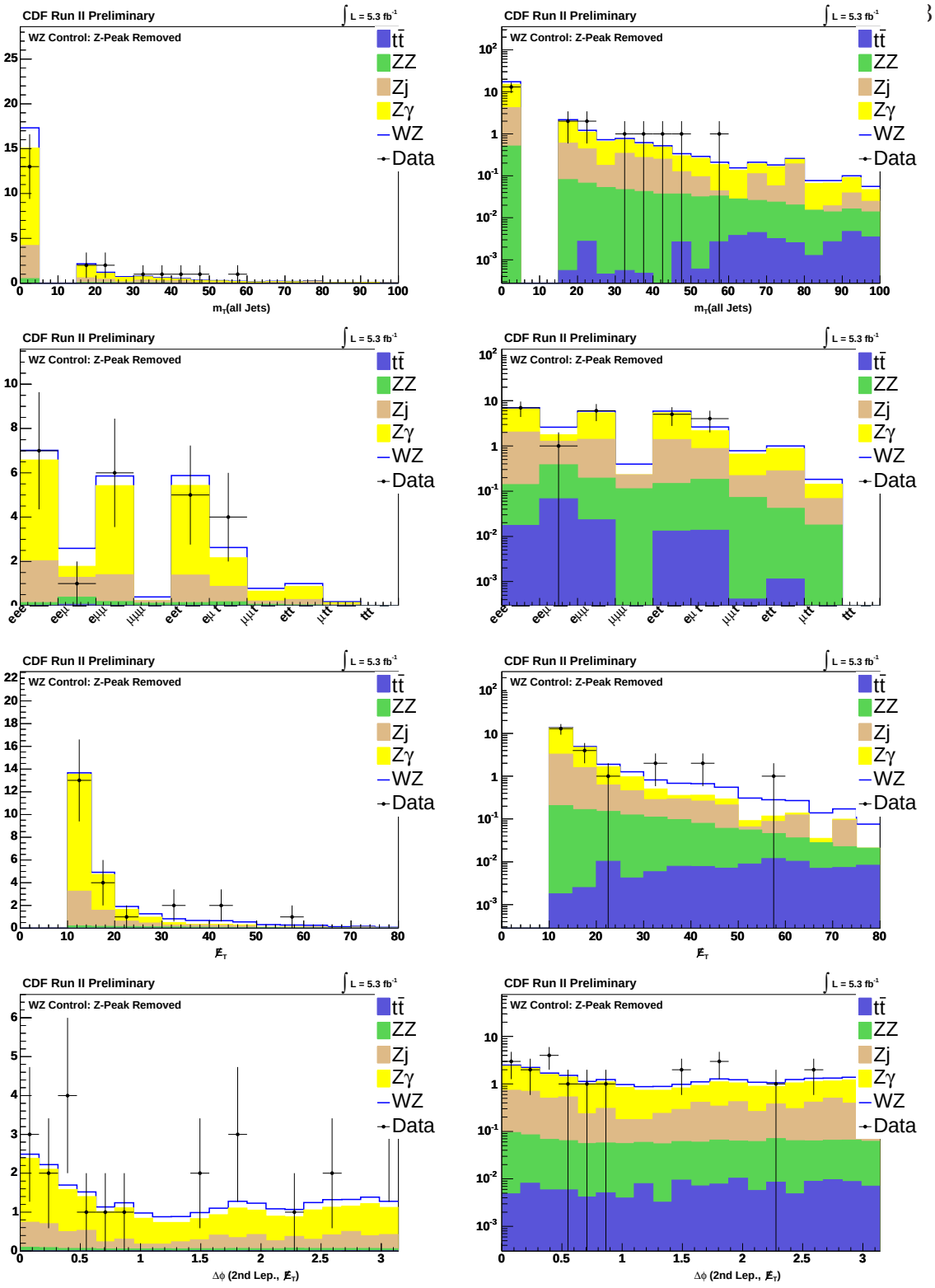

Figure 15: No Z-Peak Control Region: $\Delta\phi$ (W-Lep., $\not\!\!E_T$), m_T (jets), lepton flavor combination, $\not\!\!E_T$, m_T (W-Lep., $\not\!\!E_T$), $\Delta\phi$ (2^{nd} Lep., $\not\!\!E_T$)

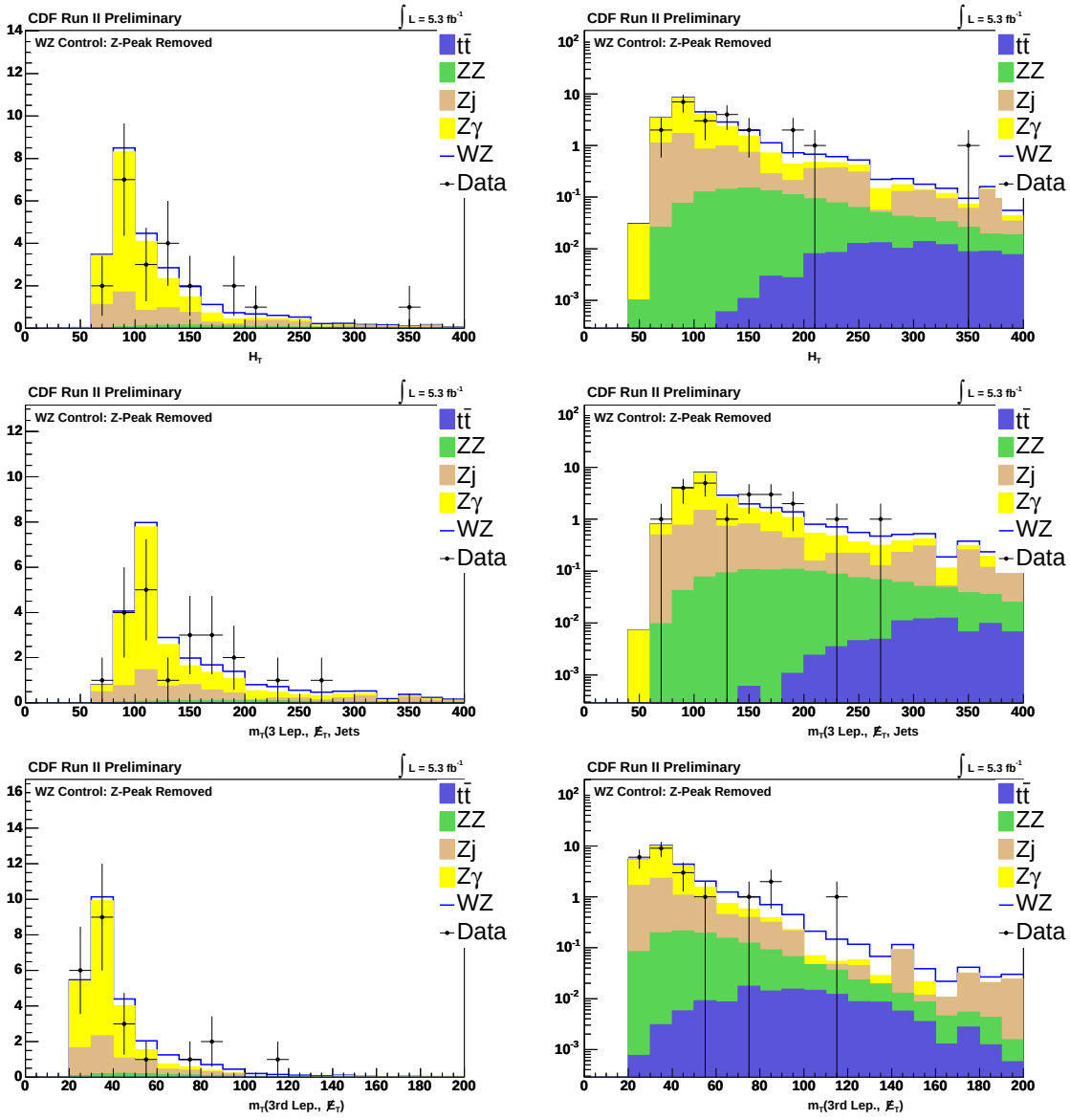

Figure 16: No Z-Peak Control Region: H_T, m_T (3^{rd} Lep., $\not\!\!E_T$, Jets), m_T (3^{rd} Lep., $\not\!\!E_T$)

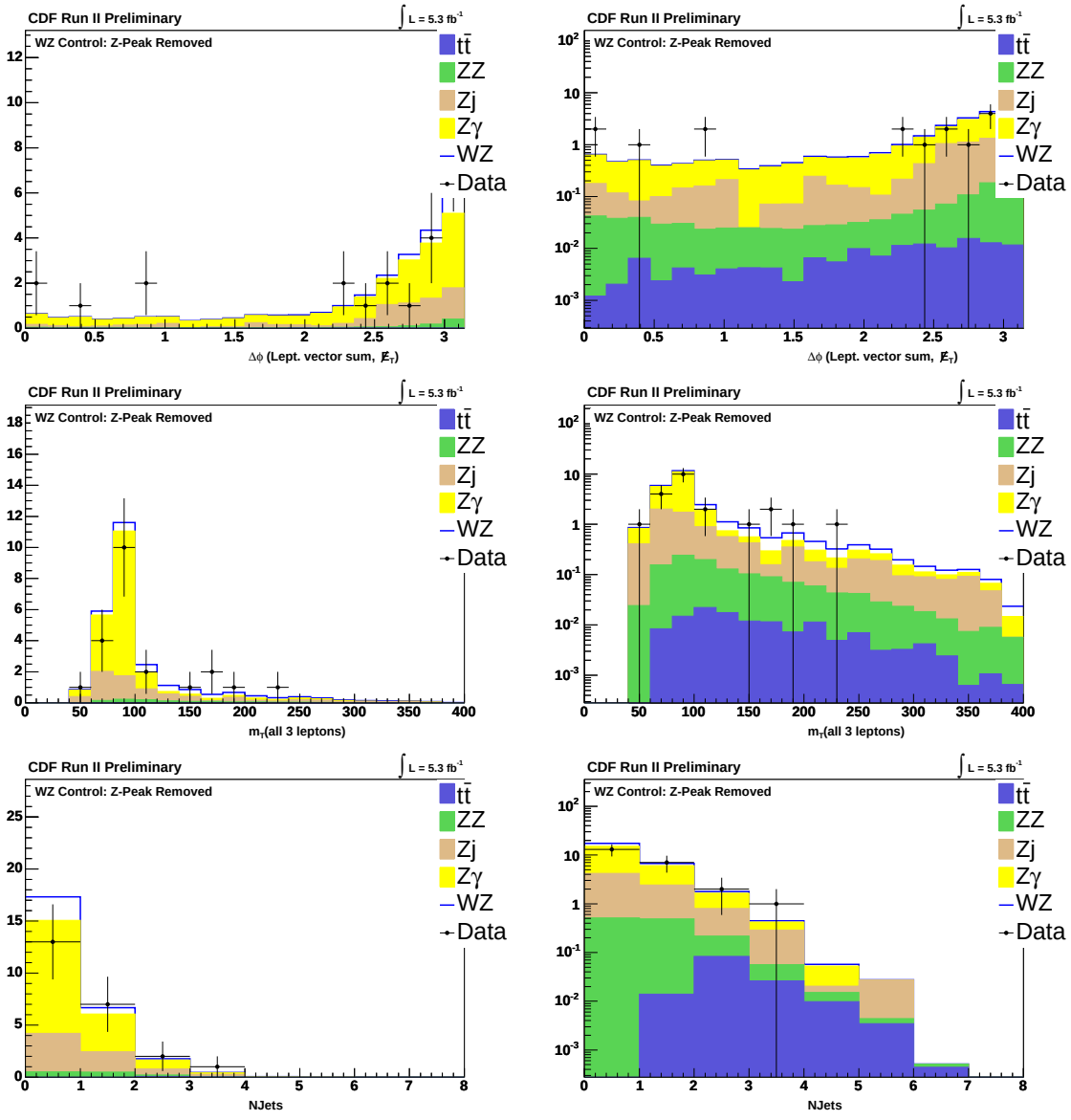

Figure 17: Z-Peak Removed Control Region: $\Delta\phi$ (vector sum of the three leptons, $\not\!\!E_T$), m_T (three leptons), NJet

Process	3.0 fb^{-1} analysis	3.6 fb^{-1} analysis	% Change
WW	12.37 pb	11.66 pb	-6%
WZ	3.65 pb	3.46 pb	-5%
$t\bar{t}$	6.7 pb	7.88 pb	+18%
Inclusive Z	k = 1.40	k = 1.38	-1.5%
Inclusive W	k = 1.40	k = 1.37	-2%

Table 8: Changes to the theoretical cross sections used in this analysis and the recent WW measurement compared to the previous analysis with 3.0 fb^{-1} of integrated luminosity. Explanations for the changes are given in the text.

B WZ Cross Section in 5.3 fb^{-1}

Many theoretical cross section predictions were updated since the 1.1 fb^{-1} analysis, as explained in CDF Note 9685 [3]. The purpose of these updates was to be consistent with the recommendations of the joint CDF/DØ Higgs combination group, but the improvements were adopted for the WW and WZ cross section measurements as well.

In particular, we increased the $t\bar{t}$ production cross section input from 6.7 pb to 7.9 pb (+18%), although this has little effect on the WZ analysis because it's contribution was already nearly negligible. We also lowered the WW and WZ diboson production cross sections from 12.37 pb to 11.66 pb (-6%) and from 3.65 pb to 3.46 pb (-5%) respectively. These changes are based on recent updates to the corresponding theoretical calculations. We also slightly adjusted our cross section inputs for inclusive W and Z production to provide a better match with NNLO calculations. In the case of Z production, the normalization is made with respect to a calculation for pure Z production (no γ^* interference). Here, we normalize based on the number of Z/γ^* events in the mass window between 66 and 116 GeV/c^2 using the theoretical factor of 1.004 which relates the number of Z/γ^* events in this mass window to the number of pure Z events over the entire mass range. In the end, we reduce our k-factor for inclusive W production from 1.40 to 1.36 (-2%).

The Z+jets contribution is determined from the data. We also slightly improved the fake rate model since 1.1 fb^{-1}. Specifically, the method of applying corrections for non-triggerable fake events improved. Previously, we had taken a standard set of corrections from the default base region, which uses events with either zero or one reconstructed jets, and applied them to all other regions. Now corrections are calculated specifically for events with zero reconstructed events. In addition, the fake rate corrections for non-triggerables applied in this version of the analysis have been determined based on our full set of inclusive W boson samples incorporating the proper weighting factors for the run-dependent and run-independent samples.

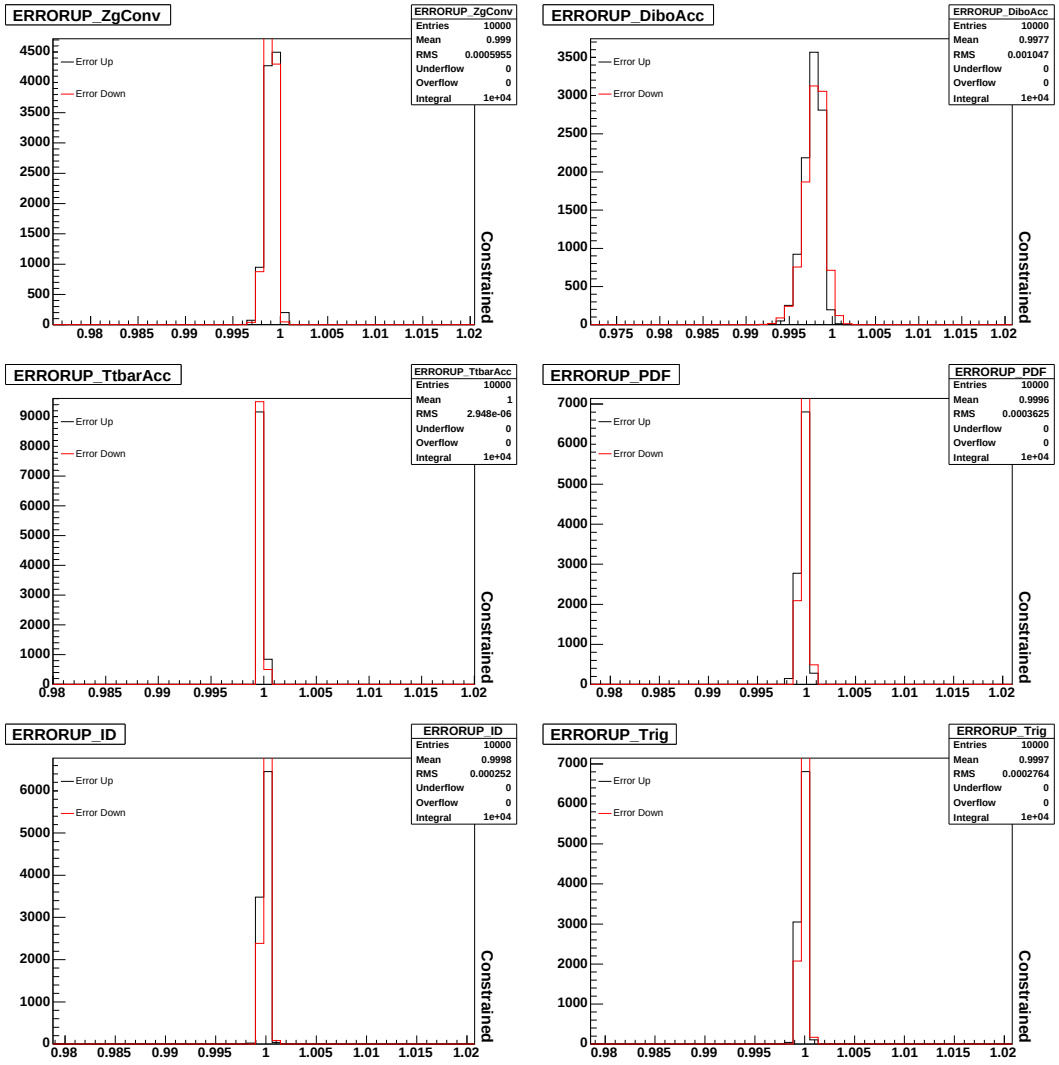

Figure 18: Fit errors for each systematic considered in the LRWZ fit.

C Psuedo-Experiment Fit Errors

This analysis uses the asymmetric errors from the fit which are returned by the MINOS algorithm. Figures 18 - 20 show the distribution of positive and negative errors for all of the constrained systematics using the 10k pseudo-experiments described in Sec. 6.1.

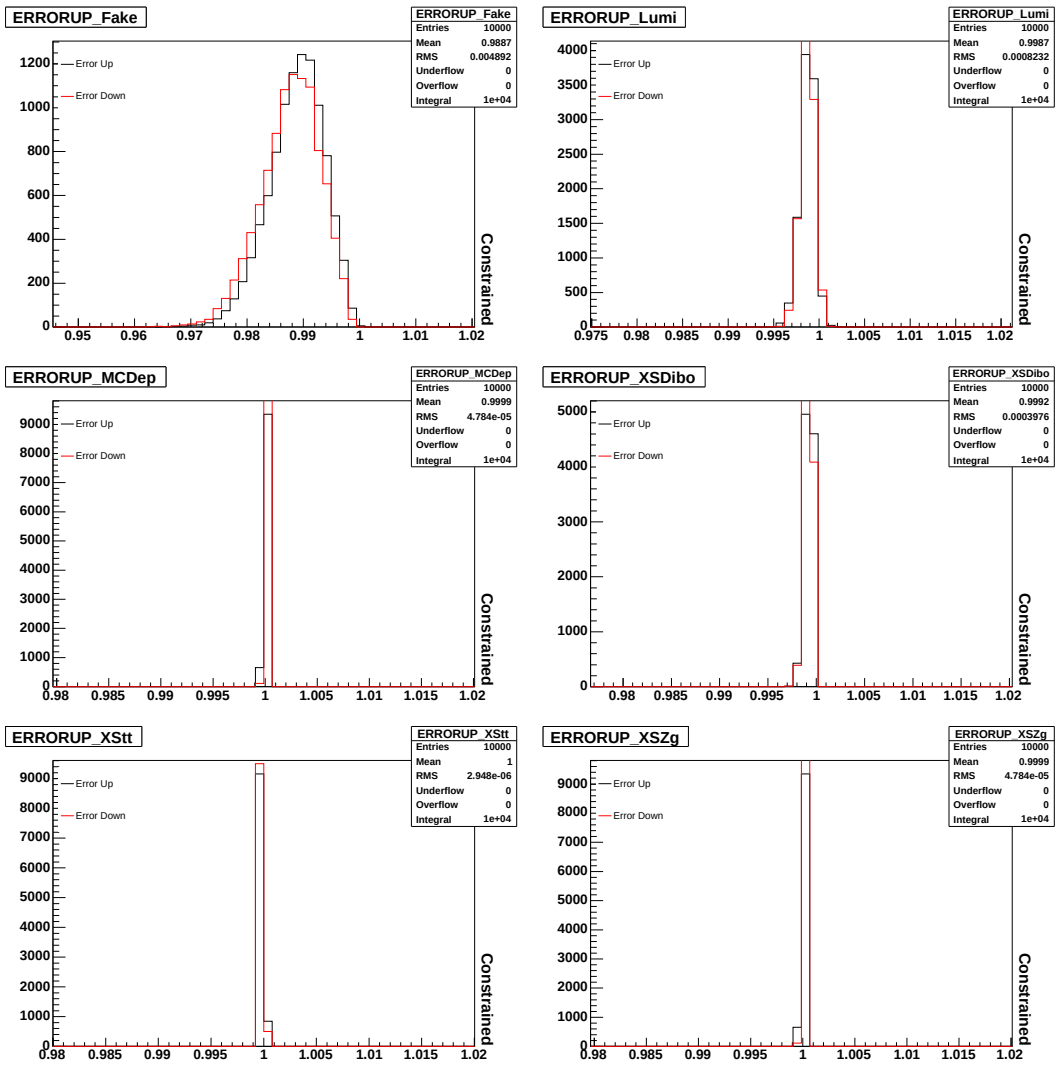

Figure 19: Fit errors for each systematic considered in the LRWZ fit.

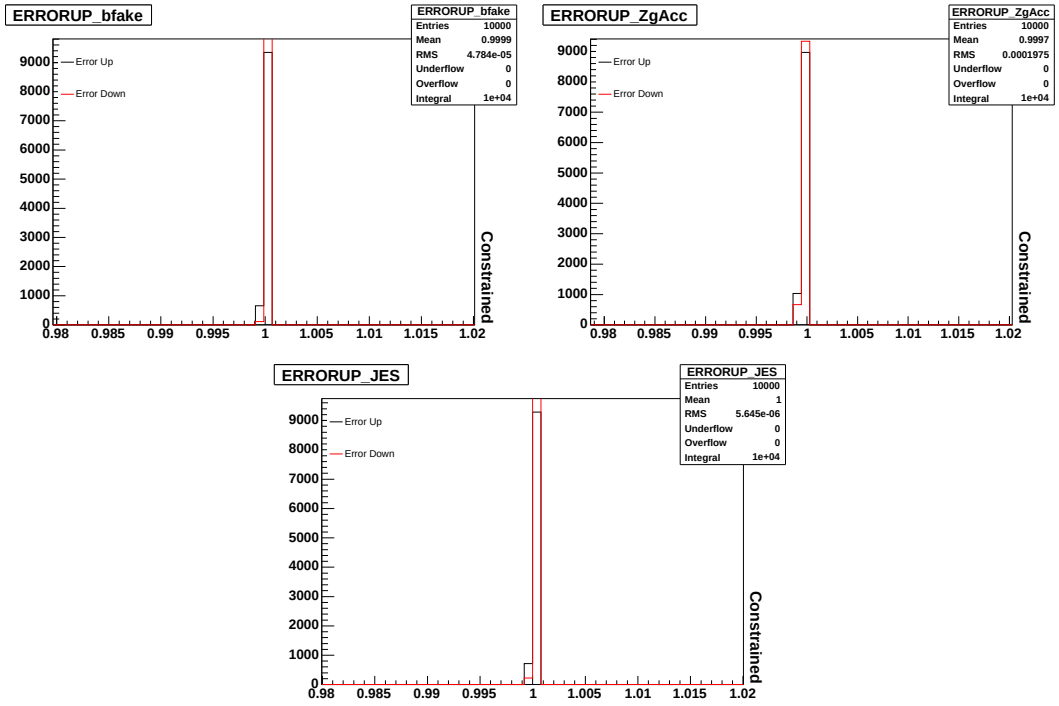

Figure 20: Fit errors for each systematic considered in the LRWW fit.

Systematic	α_{WZ}	Positive Error	Negative Error
No Syst.	1.0662884	0.1970546	0.1768465
ZgConv	1.0662481	0.1970654	0.1768553
DiboAcc	1.0582665	0.2382274	0.2212017
ttAcc	1.0662884	0.1970547	0.1768465
PDF	1.0655171	0.2003392	0.1789047
ID	1.0658904	0.1988512	0.1779732
Trig	1.0658159	0.1990489	0.1781011
Fake	1.0632795	0.1970638	0.1779794
Lumi	1.0634136	0.2117762	0.1866827
MCDep	1.0662859	0.1970553	0.1768470
XSDibo	1.0659908	0.1971662	0.1769471
XStt	1.0662884	0.1970547	0.1768465
XSZg	1.0662859	0.1970553	0.1768470
bfake	1.0662884	0.1970548	0.1768466
ZgAcc	1.0662762	0.1970579	0.1768492
JES	1.0662883	0.1970547	0.1768465
All Syst.	1.0499676	0.2564898	0.2126826

Table 9: Results from fit to data when using only the systematic given.

D Individual Systematic Effects

Here we present a study of how each systematic effects the estimated error. One systematic is included in the fit at a time to gauge which may have the largest effect on the error. 10,000 pseudo-experiments are run for each individual scenario. See table 9. The top line uses no systematic errors and so reflects Poisson statistical error only. The bottom line is the previously quoted fit result when all systematic errors are properly in place. This table clearly shows that the two most significant sources of systematic error are the diboson acceptance "DiboAcc" and luminosity "Lumi."